ELSEVIER

Journal of Magnetism and Magnetic Materials 242–245 (2002) 512–514

Journal of magnetism and magnetic materials

www.elsevier.com/locate/jmmm

Compensation of magnetostatic interactions in magnetic tunnel junctions with artificial antiferromagnets

T. Dimopoulos[a,*], C. Tiusan[a], Y. Henry[a], V. da Costa[a], K. Ounadjela[a], H.A.M. van den Berg[b]

[a] *Institut de Physique et Chimie des Matériaux de Strasbourg, 23 rue du Loess, 67037 Strasbourg, France*
[b] *Siemens AG, ZT MF1, Paul Gossenstrasse 100, Erlangen D-91052, Germany*

Abstract

We study the magnetostatic coupling between the magnetically hard and soft electrodes of tunnel junction devices employing artificial antiferromagnetic structures as hard subsystems. The coupling is found to depend drastically on the thickness and the stacking sequence of the ferromagnetic layers of the artificial antiferromagnet. By adjusting these two parameters we can cancel out the net magnetostatic coupling.

Keywords: Tunneling; Magnetic coupling interlayer; Magnetization ripples

Following the discovery of large tunnel magnetoresistance (TMR) at room temperature [1], magnetic tunnel junctions (MTJs) have become very promising for memory and sensor applications. MTJs basically consist of two ferromagnetic electrodes of different coercivities separated by a thin insulating barrier. The conduction of electrons through the barrier is spin dependent and, thus, modulated by the relative orientation of the magnetization of the two electrodes.

Among the alternatives for a magnetically hard electrode is the artificial antiferromagnet (AAF) [2,3]. The AAF structure consists of two ferromagnetic (FM) films of different thicknesses, antiferromagnetically (AF) coupled through an intermediate non-magnetic spacer layer. The AAF behaves, ideally, as a magnetic block with a reduced magnetic moment and an enhanced rigidity compared with the single FM layers entering the AAF's structure. The rigidity amplification is given by the Q factor

$$Q = (M_1 t_1 + M_2 t_2)/|M_1 t_1 - M_2 t_2|, \quad (1)$$

where M_i and t_i $(i = 1, 2)$ are, respectively, the saturation magnetization and thickness of the ferromagnetic layers that form the AAF.

In this paper we examine how, by adjusting the thickness and the stacking sequence of the AAF layers we can influence the coupling originating from magnetostatic interactions between the AAF and the soft electrode.

The junctions are sputtered on Si(1 1 1) substrates. A buffer trilayer of Cr (1.6 nm)/Fe(6 nm)/Cu(30 nm) provides a good seed system for extremely smooth interfaces (5 Å peak-to-peak after the barrier's formation) and optimized magnetic properties of the junctions. [3] We continue with the deposition of the $Co_{50}Fe_{50}/Ru/Co_{50}Fe_{50}$ AAF followed by the formation of the Al oxide tunnel barrier by plasma oxidation of a metallic Al film. The thickness of the barrier after oxidation is 20 Å. The soft subsystem consists of a CoFe(1 nm)/Fe(6 nm) bilayer, capped with Cu(5 nm)/Cr(3 nm). Junctions are patterned in areas of $20 \times 20\ \mu m^2$.

The AAF structures employed in the tunnel devices are presented in Table 1. The terms 'normal' and 'inverse AAF' relate to the stacking sequence of the artificial antiferromagnet. In the case of the normal (inverse) AAF, the thicker (thinner) layer is in contact with the barrier. All AAFs have the same Q value $(Q = 3)$.

*Corresponding author. Tel.: +33-388-10-7084; fax: +33-388-10-7249.

E-mail address: thdimop@ipcms.u-strasbg.fr (T. Dimopoulos).

0304-8853/02/$ - see front matter
PII: S0304-8853(01)01088-5

Table 1
Description of the AAF systems incorporated in the tunnel junction devices

AAF	Structure	Type
AAF1	CoFe (1 nm)/Ru(0.8 nm)/CoFe(2 nm)	Normal
AAF2	CoFe (4 nm)/Ru(0.8 nm)/CoFe(2 nm)	Inverse
AAF3	CoFe (2 nm)/Ru(0.8 nm)/CoFe(1 nm)	Inverse

The types of magnetostatic coupling existing in the present junctions are the orange peel ferromagnetic coupling due to the correlated FM metal interfaces adjacent to the barrier [4,5] and the coupling due to magnetization fluctuations (MF) inside the magnetic layers constituting the junction (as will be discussed later) [6]. As a result, an additional offset field is acting on the soft electrode's magnetization, which is written as

$$H_{\mathrm{tot}} = H_{\mathrm{N}} + H_{\mathrm{MF}}. \quad (2)$$

With the assumption of infinite thicknesses of the hard and soft electrodes and a sinusoidal, conformal interface roughness, the following equation applies for the offset field due to the orange peel coupling [4]:

$$H_{\mathrm{N}} = \pi^2 h^2 M_{\mathrm{H}}/(\sqrt{2}\lambda t_{\mathrm{SE}})\exp(-2\pi\sqrt{2}t_{\mathrm{B}}/\lambda), \quad (3)$$

where h and λ are, respectively, the amplitude and wavelength of the interfacial waviness, M_{H} is the saturation magnetization of the hard electrode, t_{SE} is the thickness of the soft electrode and t_{B} the thickness of the barrier. Eq. (3) assumes interaction only between the magnetic charges at the FM metal/barrier interfaces. In our case, the CoFe AAF layers employed, being very thin, we have to take the algebraic sum of the offset fields resulting from the magnetic charges distributed at the interfaces 2–5 of the AAF, as sketched in Fig. 1 (for a normal AAF) [7]. The offset fields due to the second and third interfaces have signs opposite to those due to the first and fourth interfaces (Fig. 1). We have calculated the net orange peel coupling for the three AAFs considered in this work, using as parameters: $h =$ 5 Å (as extracted from AFM and TEM images), $\lambda =$ 10 nm (extracted from TEM images), $M_{\mathrm{H}} = 1910$ emu/cc (saturation magnetization for CoFe) and $t_{\mathrm{B}} =$ 2 nm. The corresponding offset fields are 6 Oe for AAF1, 6 Oe for AAF2 and 3 Oe for AAF3. However, note that the model used certainly overestimates the orange peel coupling as it assumes that the magnetization of the FM layers is rigid, uniform and parallel to the field axis [4], which is not the case for polycrystalline materials.

In Fig. 2 we present rotating field and minor TMR curves corresponding, respectively, to the rotation and reversal of the soft layer's magnetization. Prior to these measurements we have saturated the junctions in 12 kOe and then decreased the field to 100 Oe. For the rotating field measurements the field (100 Oe) was successively

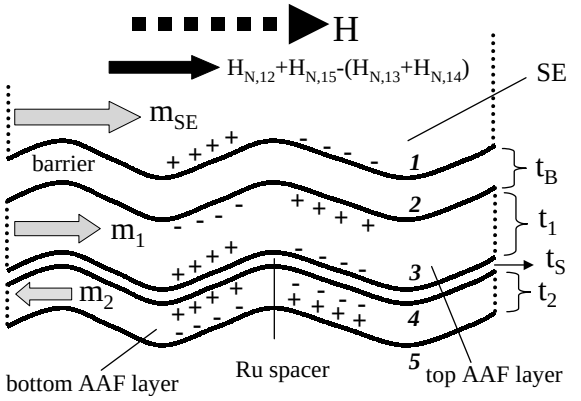

Fig. 1. Schematic representation of the interfaces of the FM layers of the AAF (labeled 2–5) and of the soft electrode, having correlated roughness profiles. $H_{\mathrm{N},1i}$ stands for the Néel offset field originating from the interaction of magnetic charges at the ith interface and at the interface between the soft electrode and the barrier (labelled 1).

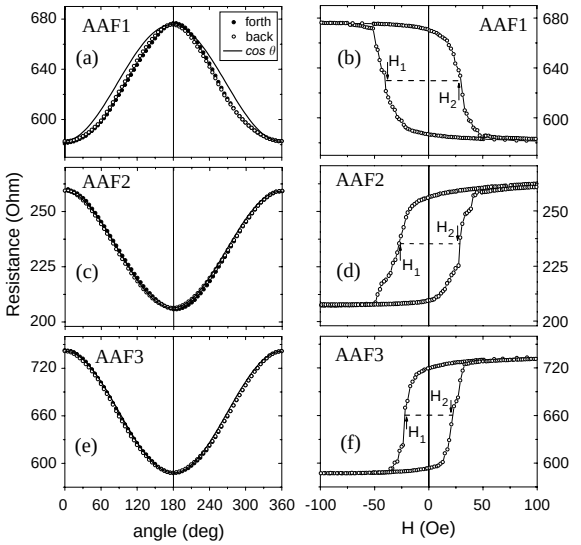

Fig. 2. Rotating field (a,c,e) and minor TMR curves (b,d,f) for junctions employing the AAF structures presented in Table 1.

rotated 360° clockwise and counterclockwise. As the applied field is only able to make the magnetization of the soft electrode rotate, the junction's resistance should follow the cosine behavior:

$$R = (R_{\mathrm{AP}} + R_{\mathrm{P}})/2 - [(R_{\mathrm{AP}} - R_{\mathrm{P}})/2]\cos\theta, \quad (4)$$

where R_{P} and R_{AP} are the junction's resistance for parallel and antiparallel alignments of the FM layers adjacent to the barrier and θ is the angle between the magnetization of the soft layer and the direction of the AAF's net moment. The above equation holds in the case where no coupling exists between the hard and the soft layers. Fig. 2(a) presents the rotating field curve in

the case of the normal AAF (AAF1). The resistance variation deviates significantly from the cosine function. Moreover, a flattening of the experimental $R(\theta)$ curve is observed around its minima (parallel alignment). This reveals that a net ferromagnetic coupling exists between the hard and the soft subsystems. From the corresponding TMR loop (Fig. 2(b)), we extracted the offset field $H_{tot} = (H_1 - H_2)/2) \sim 5$ Oe. In contrast, we can see in Fig. 2(c)–2(f) that there is almost no coupling in the case of the junctions employing the inverse AAF2 and AAF3, despite the fact that the orange peel coupling is calculated to be the same for AAF1 and AAF2.

In polycrystalline ferromagnetic layers, as in the present case, a distribution of local anisotropy axes exists, which is determined by the lateral correlation length within the grains constituting each layer. As the field is decreased from saturation, the magnetization in each of these regions relaxes towards the local anisotropy axis. This tendency is hindered by the intralayer ferromagnetic coupling, though it is definitely significant for systems without strong uniaxial anisotropy, like the systems involved in this study. Magnetic force microscopy (MFM) was used to visualize the magnetization configuration in the ferromagnetic layers of the AAF in the remanent state. The MFM image of Fig. 3(b), recorded in phase detection mode with a perpendicularly magnetized tip (hence sensing the perpendicular-to-plane component of the stray field), clearly reveals black/white contrasts almost perpendicular to the average magnetization direction. These correspond to magnetic charge distributions associated with local magnetization divergences (ripples) as sketched in Fig. 3(a) (gray-colored regions). The magnetic charges

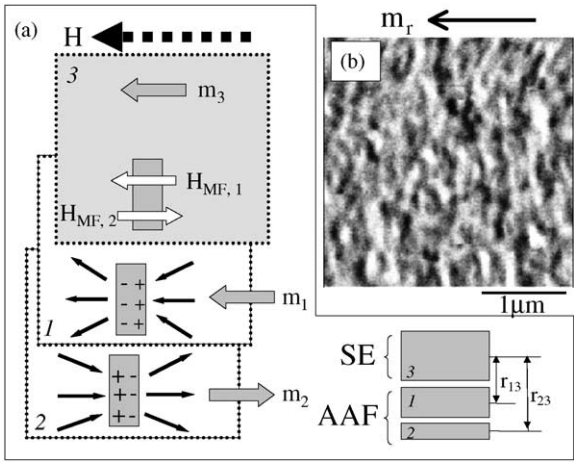

Fig. 3. MFM image (b) and schematic representation (a) of the ripple structure developed in the AAF layers, labeled 1 and 2, at the remanent state, in the case of AAF1. $H_{MF,1}$ and $H_{MF,2}$ are the stray fields sensed by the soft electrode (labeled 3), originating from the magnetic fluctuations in the first and second AAF magnetic layers, respectively.

of opposite polarity are separated by a typical distance of ~ 100 nm. Due to the interlayer AF coupling between the FM layers of the AAF the charges in a given layer are mirrored in the other one (see Fig. 3(a) and Ref. [3]).

The soft electrode is subjected to the stray fields originating from these charges. Importantly, the stray fields arising from the AAF layer which is closer to the soft electrode always give rise to a FM coupling (adding to the orange peel coupling), while those arising from the other AAF layer always result in an AF coupling (counteracting the orange peel coupling), irrespective of the stacking sequence. Therefore, the total MF offset field acting on the soft electrode is given by

$$H_{MF} \sim t_2/r_{23} - t_1/r_{13}, \quad (5)$$

where the distances $r_{23,13}$ are defined in Fig. 3(a). This expression clearly shows that for junctions with normal AAF ($t_2 > t_1$, $r_{23} < r_{13}$), such as that containing AAF1, the net MF coupling is always ferromagnetic and thus adds systematically to the orange peel coupling. However, expression 5 also suggests that by placing that of the two AAF FM layers with the smaller thickness closer to the soft electrode ($t_2 < t_1$), i.e. by using an inverse AAF scheme, and by adjusting the thicknesses t_1 and t_2, one might be able to control both the intensity and the sign of the net MF coupling. In particular, choosing appropriate thicknesses we can generate an antiferromagnetic MF coupling that fully compensates the (ferromagnetic) orange peel coupling. This is what is more or less achieved in the junctions containing AAF2 and AAF3, which exhibit a zero overall coupling.

The authors would like to thank Dr. M. Hehn, Dr. C. Meny, M. Acosta, G. Wurtz and G. Ehret. This work was partially supported by the European Community Brite Euram project 'Tunnelsense' (BRPR98-0657) and the Training and Mobility of Researchers programme of the EC through the 'Dynaspin' project (FMRX-CT97-0124).

References

[1] J.S. Moodera, L.R. Kinder, T.M. Wong, R. Meservey, Phys. Rev. Lett. 74 (1995) 3273.
[2] H.A.M. van den Berg, W. Clemens, G. Gieres, G. Rupp, M. Vieth, J. Wecker, S. Zoll, J. Magn. Magn. Mat. 165 (1997) 524.
[3] C. Tiusan, T. Dimopoulos, K. Ounadjela, M. Hehn, H.A.M. van den Berg, Y. Henry, V. Da Costa, Phys. Rev. B 61 (2000) 580.
[4] L. Néel, C. R. Acad. Sci. 255 (1962) 1676.
[5] S. Demokritov, E. Tsymbal, P. Grünberg, W. Zinn, I.K. Schuller, Phys. Rev. B 49 (1994) 720.
[6] C. Tiusan, T. Dimopoulos, L. Buda, V. da Costa, K. Ounadjela, M. Hehn, H.A.M. van den Berg, J. Appl. Phys. 89 (2001) 6811.
[7] J. Zhang, R.M. White, IEEE Trans. Magn. 32 (1996) 4630.